Fire regimes and variability in aboveground woody biomass in miombo woodland

Makoto Saito, Sebastiaan Luyssaert, Ben Poulter, Mathew Williams, Philippe Ciais, Valentin Bellassen, Casey M. Ryan, Chao Yue, Patricia Cadule, Philippe Peylin

▶ **To cite this version:**

Makoto Saito, Sebastiaan Luyssaert, Ben Poulter, Mathew Williams, Philippe Ciais, et al.. Fire regimes and variability in aboveground woody biomass in miombo woodland. Journal of Geophysical Research: Biogeosciences, 2014, 119 (5), pp.1014. 10.1002/2013JG002505 . hal-01138869

RESEARCH ARTICLE

Key Points:
- Aboveground biomass is controlled by fire regimes
- Current fire management results in degradation of miombo woodland
- Future climate change has a positive effect on biomass of miombo woodland

Fire regimes and variability in aboveground woody biomass in miombo woodland

Makoto Saito[1,2], Sebastiaan Luyssaert[1], Ben Poulter[1,3], Mathew Williams[4], Philippe Ciais[1], Valentin Bellassen[5], Casey M. Ryan[4], Chao Yue[1], Patricia Cadule[1], and Philippe Peylin[1]

[1]Laboratoire des Sciences du Climat et de l'Environnement, CEA-Orme des Merisiers, Gif-sur-Yvette, France, [2]Center for Global Environmental Research, National Institute for Environmental Studies, Tsukuba, Japan, [3]Institute on Ecosystems and Department of Ecology, Montana State University, Bozeman, USA, [4]School of Geosciences, Crew Building, Kings Building, University of Edinburgh, Edinburgh, UK, [5]CDC Climat, Paris, France

Abstract This study combined a process-based ecosystem model with a fire regime model to understand the effect of changes in fire regime and climate pattern on woody plants of miombo woodland in African savanna. Miombo woodland covers wide areas in Africa and is subject to frequent anthropogenic fires. The model was developed based on observations of tree topkill rates in individual tree size classes for fire intensity and resprouting. Using current and near-future climate patterns, the model simulated the dynamics of miombo woodland for various fire return intervals and grass cover fractions, allowing fire intensity to be estimated. There was a significant relationship between aboveground woody biomass and long-term fire regimes. An abrupt increase in fire intensity and/or fire frequency applied as a model forcing led to reduced long-term average aboveground woody biomass and mean tree size. Fire intensity increased with increasing living grass biomass (which provides increased flammable fuel), thereby affecting the relationship between fire regime and tree size, creating a demographic bottleneck on the route to tree maturity. For the current fire regime in miombo woodland, with a fire return interval of about 1.6–3 years, the model-predicted fire intensity lower than 930–1700 kW m^{-1} is necessary to maintain today's aboveground woody biomass under current climate conditions. Future climate change was predicted to have a significant positive effect on woody plants in miombo woodland associated with elevated CO_2 concentration and warming, allowing woody plants to survive more effectively against periodic fires.

1. Introduction

Savanna ecosystems cover 15% of the Earth's ice-free land surface and are the dominant land cover in Africa with 35% coverage [*Loveland et al.*, 2000]. Savanna ecosystems occur under a broad range of environmental conditions [*Ciais et al.*, 2011], and as a consequence, their appearance varies due to differences in species composition and tree density. Tree cover is predominantly constrained by precipitation in arid and semiarid savannas [*Sankaran et al.*, 2005] but is regulated by fire in mesic savannas where precipitation is sufficient for the establishment of forests [*Bond et al.*, 2005; *Mayer and Khalyani*, 2011; *Staver et al.*, 2011]. Fire typically prevents trees reaching maturity and favors the development of a grass layer, generating the characteristic landscape of savannas, codominance of grasses and trees [*Higgins et al.*, 2000; *D'Odorico et al.*, 2006]. During the dry season, this grass layer also provides a fuel that makes the entire ecosystem more prone to fire, thereby maintaining a low tree density.

Savannas are thought to show high sensitivity to atmospheric CO_2 level and climate regime [*Sala et al.*, 2000] and have the potential to shift to a forested state in a future high-atmospheric-CO_2 world [*Higgins and Scheiter*, 2012]. In contrast, future climate is predicted to increase the likelihood of savanna fires as a result of changes in maximum temperature and humidity [*Williams et al.*, 2001; *Pitman et al.*, 2007], a process that would act to reduce or suppress tree cover. It remains unknown whether the current state of savanna tree cover will be maintained or if it will shift in response to elevated atmospheric CO_2 concentrations and subsequent changes in climate.

In the early 2000s, 60%–70% of the global total burnt area was located in Africa. Almost all of these African wildfires occurred in savannas in tropical and subtropical regions [*Roy et al.*, 2008]. Although few data are available about causes of fire in Africa, many fires are probably caused by human activities [*Frost*, 1999; *Archibald et al.*, 2009], such as cultivation, deforestation, and fuel wood collection [*Abbot and Homewood*, 1999; *Lambin et al.*, 2003; *Mouillot and Field*, 2005]. These activities often support subsequent development

of agriculture, infrastructure, and the regional economy, but other interventions are still required to secure these benefits [*Fisher*, 2010].

These human-induced fires burn African savannas at fire return intervals of 1–3 years [*Barbosa et al.*, 1999; *Van der Werf et al.*, 2003] and can locally result in degradation of the aboveground biomass pool [*Ryan et al.*, 2012]. The destruction of large areas of savanna by human-induced fire involves the risk that the current stable state of these ecosystems could suddenly switch into an alternative stable state [*Scheffer et al.*, 2001]. In the case of mesic savannas a further increase in fire frequency or fire intensity is expected to reduce woody biomass in favor of grassy biomass. In turn, more grassy biomass may result in reduced resilience to future climate change and diminish the ecosystem services and resources currently supporting high population growth.

Assessing the effect of fire disturbance on savanna ecosystems and climate and understanding the possibilities and limitations of human-fire interactions with respect to the woody biomass are needed to ensure preservation of the ecosystem on which a large proportion of the African population depends. However, few research efforts have been focused on this issue [*Andersen*, 1991; *Peterson and Reich*, 2001; *Hély et al.*, 2003].

In this study, we quantify the relative importance of fire regime and climate change in regulating aboveground woody biomass in miombo woodland under current and near-future climate conditions. Miombo woodland is a savanna that spreads extensively over Africa, covering about 2.7 million km^2 in southern, central, and eastern Africa [*Frost*, 1996]. It is generally dominated by *Brachystegia* and *Julbernardia* tree species but with a continuous grass layer beneath. We aim to assess whether the woody biomass of miombo woodland will be maintained or degraded under future climate change. This analysis employs a global ecosystem model that has been further developed to represent fires and their impact on tree cover. The model is calibrated with an ensemble of in situ measurements made in miombo woodland [*Williams et al.*, 2008; *Ryan and Williams*, 2011].

2. Methods and Data

2.1. Study Region

This study extends a process-based ecosystem model using data from two sites in miombo woodland, located in N'hambita community within the buffer zone of Gorongosa National Park, in Sofala Province, Mozambique. Site 1 is a collection of abandoned agricultural sites [*Williams et al.*, 2008], originally cleared for agriculture but then deserted, allowing trees and shrubs to regrow for 2–25 years (18.58°S, 34.10°E). Site 2 is an area of experimentally burnt miombo woodland (18.98°S, 34.18°E) [*Ryan and Williams*, 2011]. Mean annual precipitation (1959–1967 and 1999–2007 at Chitengo, 25 km from the burnt site) is 850 mm, which is high for savanna vegetation; however, all the rain falls in the summer months of October to April, leaving a 5 month dry season during which fires occur. The soils are well-drained sandy loams or sandy silt loams. The data on basal area, tree density, and distribution of stem diameters were collected by field survey at the abandoned agricultural sites in June 2005. Details of the fire behavior and tree topkill rate in the experimentally burnt miombo woodland considered in this study are given by *Williams et al.* [2008] and *Ryan and Williams* [2011].

2.2. Modeling Framework

In the past 15 years several terrestrial biosphere models focused on savanna ecosystems have been constructed to quantify the sensitivity of such ecosystems to ecological processes, including landscape processes such as fire and grazing [e.g., *Simioni et al.*, 2000; *Leriche et al.*, 2001]. Fire dynamics in savanna ecosystems have been predicted using various approaches, such as the cellular automaton (CA) model [*Berjak and Hearne*, 2002], a coupled atmosphere-fire model [*Clark et al.*, 2004], and the fire risk assessment algorithm (FIRA) algorithm [*Mbow et al.*, 2004]. The forest savanna transgression (FORSAT) model [*Favier et al.*, 2004], which is an expanded version of the CA model, was developed to study the transition of the boundaries between forests and savannas due to human-induced fires and environmental variability. Furthermore, a matrix population model has been used to study the effect of fire on the population dynamics of savanna plant species [*Silva et al.*, 1991; *Hoffmann*, 1999]. The coexistence of grasses and trees in a savanna ecosystem under various conditions of rainfall and fire has been modeled using empirical equations linking rainfall to plant productivity [*Higgins et al.*, 2000]. Finally, *Scheiter and Higgins* [2009] developed a dynamic global vegetation model including topkill by fire for tropical vegetation, and the model successfully simulated current vegetation patterns in Africa.

This study builds on a global large-scale land surface model, ORCHIDEE-FM (Organizing Carbon and Hydrology in Dynamic Ecosystems-forest management module) [*Bellassen et al.*, 2010], and a process-based ecosystem model, with the SPITFIRE (spread and intensity of fire) regime model [*Thonicke et al.*, 2010] to simulate the fire-driven stand dynamics in miombo ecosystems. The version of the model used in this study is designed and parameterized specifically for miombo woodland, although given its structure and objectives, it remains applicable to other biomes.

ORCHIDEE-FM includes a module for plant functional types (PFTs) of woody trees that adds to the original ORCHIDEE [*Krinner et al.*, 2005] by simulating forest stand growth and mortality based on natural competition and/or forest management thinning and harvest rules. In ORCHIDEE-FM, the woody net primary production (NPP) of an average forest is divided between individual trees following the principles that at the stand level, more carbon is allocated to large individuals than to small individuals [*Dhôte and Hervé*, 2000]. Also, beyond a critical density, individual trees compete with each other for resources, causing natural mortality, i.e., self-thinning [*Yoda et al.*, 1963]. Seasonal processes in the carbon dynamics of grass and crop PFTs are already simulated by ORCHIDEE [*Krinner et al.*, 2005]. SPITFIRE calculates the probability of additional tree mortality due to fire from the probability of ignition [*Nesterov*, 1949], the rate of spread of free-burning fire [*Rothermel*, 1972], the amount of wood and grasses with a favorable moisture content to fuel fire, bark thickness, and crown height.

Coupling ORCHIDEE-FM with SPITFIRE results in a prognostic stand growth model that can simulate the probability of individual trees burning and dying, or surviving (i.e., young trees with thin bark have a higher probability of burning than mature trees with thick bark), and can simulate the subsequent competition from the growth of trees which have survived the fire, and resprouting of the topkilled trees by the fire, as described below. In the model, no temporal change in tree/grass cover associated with fire occurs in individual model runs. Eight different vegetation fractions of living grass are applied in the simulations to compensate the lack of vegetation cover dynamics.

The forest growth and management module (FM) and the fire module (SPITFIRE) were parameterized for miombo forest using data from the sites described above. The observations from the abandoned agricultural sites were used to parameterize regrowth of trees after clear-cutting and competition between trees in miombo woodland. The data from the experimentally burnt site were used to calibrate the stochastic frequency and intensity of fires. Biogeochemical parameters of PFTs for tropical dry-season deciduous trees and natural C4 grass in ORCHIDEE were used.

Our modeling approach for miombo woodland is similar to that used in the fire and landscape tree model for tropical savannas (FLAMES) model [*Liedloff and Cook*, 2007], which is a process-based model being designed for examination of tree population dynamics in Australian savanna. It considers detailed fire processes and subsequent tree mortality and resprouting in a stand. FLAMES successfully modeled tree population dynamics in Australian savanna by taking into account the interactive effects of fire regime and rainfall variability. Our model differs to FLAMES through its more detailed and explicit representation of the development of individual trees and variability of deadwood fuel pools, which enable the model to predict fire regimes and their impact on tree cover. The average aboveground woody biomass and fire regimes were calculated from an ensemble of 500 year simulations (see Appendices A and B).

2.3. Overview of Model Setup

ORCHIDEE was forced by observed and modeled climatological drivers at a half-hourly time step (see below). Photosynthesis and all physical variables, including water and energy fluxes, were also calculated at a half-hourly time step. At the end of every day the SPITFIRE module simulated fire intensity, I_{fire}, and total burnt area, A_b, following a semiempirical fire regime model [*Rothermel*, 1972] accounting for fuel stocks and meteorological conditions (Appendix B in the supporting information). Mean fire return interval within a given area, RI_{fire}, was estimated by accumulating A_b over the entire simulation period. To test the relationship between fire regimes and carbon dynamics of miombo woodland, RI_{fire} was changed by multiplying A_b by various scaling factors, leading to changes in I_{fire} and carbon stocks. In our approach, the seasonal change in fire regime is the outcome of daily aggregated changes in fuel stocks and distribution and the daily averages of the moisture content of the fuels (Appendix B1). In contrast, the FM module was run only at the end of each year to update the number of trees and their individual diameter change by accounting for trees killed by fire (Appendix B3), for resprouting (Appendix C) and for self-thinning (Appendix A2) over the whole year. The FM module distributes NPP to the surviving individuals and newly established sprouts. The module

Table 1. World Climate Research Program's (WCRP's) CMIP3 Models Used in This Study[a]

Organizations/Groups	Model Designation	Pr/Ta	SH
National Center for Atmospheric Research	CCSM3	○	
Canadian Centre for Climate Modeling	CGCM3.1	○	○
CSIRO Atmospheric Research	CSIRO-Mk3.5	○	○
Max Planck Institute for Meteorology	ECHAM5	○	
Meteorological Institute of the University of Bonn (MIUB), Meteorological Research Institute of KMA (METRI) and Model and Data group (M and D)	ECHO-G	○	
U.S. Department of Commerce/NOAA/Geophysical Fluid Dynamics Laboratory	GFDL-CM2.1	○	
NASA/Goddard Institute for Space Studies	GISS-ER	○	○
Institute for Numerical Mathematics	INM-CM3.0		○
Institut Pierre Simon Laplace	IPSL-CM4	○	○
National Center for Atmospheric Research	PCM	○	
Hadley Centre for Climate Prediction and Research, Met Office	UKMO-HadCM3	○	
Hadley Centre for Climate Prediction and Research, Met Office	UKMO-HadGEM1	○	

[a]Open circles indicate data availability for precipitation/air temperature (Pr/Ta) and specific humidity (SH). Organizations/groups abbreviations: CSIRO = Commonwealth Scientific and Industrial Research Organisation, KMA = Korea Meteorological Administration, METRI = Meteorological Research Institute.

updates the distributions of individual diameters and heights in the population from the calculated basal area increment for individuals.

Subsequently, all diameters are allocated to discrete bins of 1 cm width. For each diameter class the probability of the annual tree topkill rate, M_{tree} (Appendix B3), and the annual mean proportionality of the scorch height, SH, to crown length, CK (Appendix: Table A3 in the supporting information), are computed cumulatively making use of the daily estimates for I_{fire} and A_b over the year.

For small trees (diameter breast high (DBH) < 10 cm), the number of trees topkilled by fire, X_i, is counted for each diameter class i by multiplying $M_{\text{tree},i}$ by the sum of the number of trees within the class. The top $X_{i\text{th}}$ trees with largest DBH are then removed from the class. For large trees (DBH $\geq$ 10 cm), $M_{\text{tree},i}$ is constant for DBH (Appendix: equation (B2) and Figure A1 in the supporting information), so X is counted by multiplication of $M_{\text{tree, 10 cm}}$ by the number of trees across all classes with DBH $\geq$ 10 cm. The distribution is then divided into X classes and the largest diameter removed from each class. The ratios of combustion to dead-fuel allocation for topkilled trees are calculated for each diameter class based on the annual mean CK. Self-thinning is subsequent to fire disturbance when the relative density index (RDI) about the onset of self-thinning is RDI > 1 (Appendix A2 and equation (A4)).

The FM module, applied annually to model competition and growth between individuals in the stand, makes use of variables calculated in both ORCHIDEE and SPITFIRE. As all modules were integrated into the ORCHIDEE code, we call this model chain ORCHIDEE-FM-SPITFIRE.

2.4. Meteorological Forcing Data

ORCHIDEE-FM-SPITFIRE requires seven climate-forcing variables: downward surface shortwave radiation (W m^{-2}), downward surface longwave radiation (W m^{-2}), air temperature (K), specific humidity (g kg^{-1}), wind speed (m s^{-1}), surface pressure (Pa), and precipitation (mm). Three years (2006–2008) of half-hourly meteorological data from Chitengo, Mozambique, were used for the simulation under current climate conditions. ERA-Interim reanalysis data [*Dee et al.*, 2011] were substituted for the unmeasured forcing variables of downward longwave radiation at the surface and surface pressure and to cover gaps in the observations.

We used the bias-corrected [*Poulter et al.*, 2010] monthly air temperature, precipitation, and specific humidity data from the World Climate Research Program's (WCRP's) Coupled Model Intercomparison Project phase 3 (CMIP3) multimodel data set [*Meehl et al.*, 2007] to produce future climate change scenarios for the study region. Air temperature and precipitation data were derived from 11 out of 24 climate models; model results lacking specific humidity as an archived output (Table 1) were excluded, leaving five models. All data were provided by the WCRP's CMIP3 experiments using atmosphere-ocean general circulation models with the Special Report on Emissions Scenarios (SRES) A2 scenario. The SRES A2 represents a high-impact scenario resulting in atmospheric CO_2 concentration of about 820 ppm by the year 2100. This

scenario allows us to depict potential impacts of climate change on miombo woodland and fire regimes in a high-atmospheric-CO_2 world. For simplicity, mean values of monthly variables of air temperature, precipitation, and specific humidity, computed from all available models, were used in this study. Future time series in air temperature, T_{FC}, with a half-hourly time step were generated by scaling the observation data, T_{obs}, by the ratio of mean future climate patterns, TC_{ft}, and current patterns, TC_{cr}, from the WCRP's CMIP3 for each month as follows:

$$T_{FC}(m, y) = T_{obs}(m, y) \times \frac{TC_{ft}(m)}{TC_{cr}(m)} \tag{1}$$

where m is month, y is year, and TC_{ft} and TC_{cr} are the monthly mean values for 2091–2100 and 2006–2008, respectively. Similarly, equation (1) was used to generate future time series in precipitation and specific humidity. Observation data of downward surface shortwave radiation, downward surface longwave radiation, wind speed, and surface pressure were used to give future climate patterns without any modification, thus assuming that there will be negligible change in climate patterns for these variables in the near future. Atmospheric CO_2 concentration was fixed at 784 ppm, the mean concentration of SRES A2 in the period 2091–2100.

2.5. Model Experiment
By repeating the 3 year observed climate, with atmospheric CO_2 concentration fixed at the level of the preindustrial period, the model was initially run for a spin-up period of about 3000 years, with FM but without fire disturbance. This spin-up was to ensure the equilibrium of each carbon pool and the presence of trees. All aboveground biomass after spin-up was clear-cut at the beginning of the first year for all simulations. The following model simulations were made:

1. The regrowth process of miombo woodland was simulated over 25 years with fire. This was to compare with observations made at the abandoned agricultural fields [*Williams et al.*, 2008].
2. The impact of various fire regimes under the current climate was assessed by running the model over a 500 year period with eight different vegetation fractions of living grass combined with 34 different empirical coefficients of mean fire duration, t_{fire} ($n = 272$) (see Appendix B2).
3. The impact of future climate was tested with a similar ensemble of simulations (8 fractions of grass $\times$ 25 t_{fire}) with current and elevated atmospheric CO_2 concentration ($n = 200$). Simulations with $RI_{fire} < 1$ yr and $RI_{fire} > 20$ yr were excluded to reduce the computation time.

Different grass fractions induce different I_{fire}, while different values of t_{fire} generate various fire return intervals, RI_{fire} (see Appendix B2). The stationarities of time series in I_{fire} and RI_{fire} over the simulation period were evaluated using an augmented Dickey-Fuller test, and all simulations were found to satisfy the stationarity criterion. In analyzing the fire experiment, an analysis of variance was performed to test the influence of RI_{fire} and I_{fire} on the aboveground woody biomass.

3. Results
3.1. Miombo Woodland Regrowth
The abandoned agricultural sites were exposed to repeated fire disturbance, but there are no records of fire intensity or fire return interval (Appendix B2) [*Williams et al.*, 2008]. The simulations were therefore guided by the ranges observed from the nearby experimentally burnt miombo woodland [*Ryan and Williams*, 2011]: $360 \leq I_{fire} \leq 3\,800$ kW m^{-1} and $1 \leq RI_{fire} \leq 5$ yr.

Under corresponding fire regimes, observed basal area (BA) is significantly correlated ($P < 0.001$) with years since abandonment (Figure 1a). The model shows a good agreement ($P < 0.001$) in BA between the observations and the median of model predictions. Tree density reaches its peak at around 10–20 years before declining, probably due to self-thinning competition (Figure 1b). The time evolution of the modeled tree density varies with fire regimes. These variations cover a large part of the observations. The median of the predicted tree density was significantly correlated with the observations ($P = 0.003$), but considering the low value of R^2 (0.29) and the large root-mean-square error, RMSE, (309 ha^{-1}), this is due to scatter in the observations. Tree density decline by self-thinning was found in 29 model runs (out of 35). The medians of BA and tree density in 25 years were 8.4 m^2 ha^{-1} and 569 ha^{-1} for observations and 7.4 m^2 ha^{-1} and 551 ha^{-1} for model predictions, respectively.
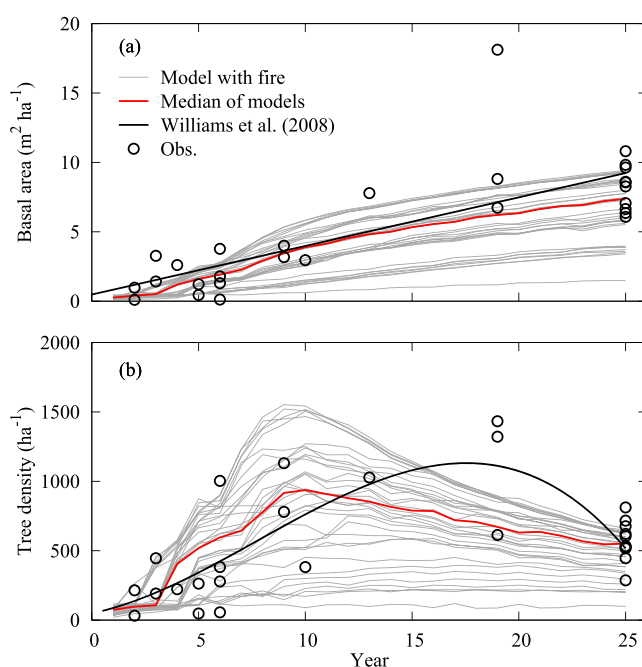
Figure 1. Temporal evolution of basal area and tree density of miombo woodland on abandoned agricultural sites under various fire regimes. (a) Basal area (m^2 ha^{-1}) and (b) tree density (ha^{-1}) of trees with DBH $\geq$ 5 cm. Open circles show observational data, and black lines are regressions by *Williams et al.* [2008]. Gray lines are the model simulations under the fire regimes of $1 \leq RI_{fire} \leq 5$ yr and $I_{fire} \leq 3800$ kW m^{-1}. Red lines are the median of the model results, which show a correlation with observations with R^2 of 0.64 and RMSE of 2.7 m^2 ha^{-1} for BA and R^2 of 0.29 and RMSE of 309 ha^{-1} for tree density. The model was run for 25 years after clear-cutting all aboveground biomass at the start of the simulation.

The resprouting process of juveniles after fire is simulated with regrowth of the trees killed by fire (see Appendix C). Overall, Figure 1 shows that the initial diameter distribution of the sprouts, and their subsequent growth in the miombo woodland, can be reproduced by our model.

3.2. Fire Regimes Under Current Climate Conditions

Fire intensity increased with less frequent fire return intervals and grass biomass ($P < 0.001$) due to increasing dead biomass pools and highly flammable living grass (Figure 2). There is a significant effect of fire regime on aboveground woody biomass (AGB) of miombo woodland ($P < 0.001$), resulting in AGB in the range of 0 to 36 Mg C ha^{-1} over various fire regimes. AGB increased with increasing RI_{fire} and with decreasing I_{fire}. The fire intensity range of 360 to 3800 kW m^{-1} observed at the experimentally burnt miombo woodland [*Ryan and Williams*, 2011] is relatively narrow, and its maximum is relatively low when compared with other studies of African savannas; e.g.,
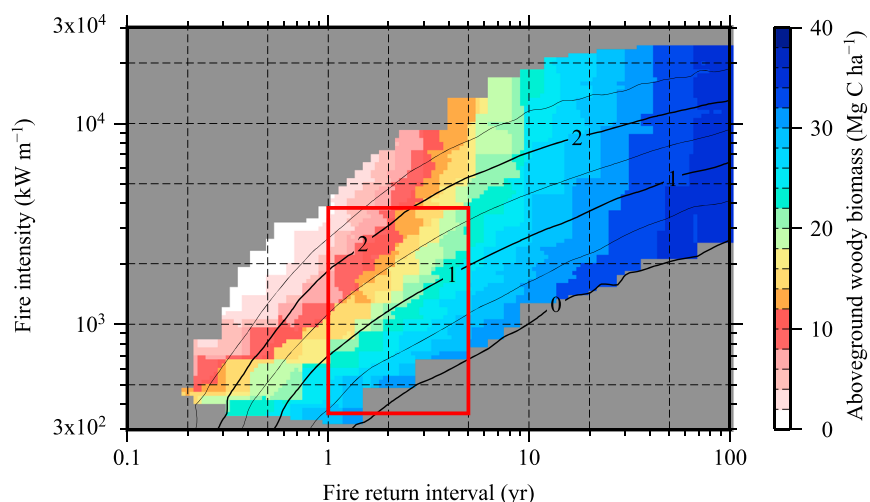
25–6553 kW m^{-1} in miombo woodland [*Hoffa et al.*, 1999], 43–9476 kW m^{-1} in grass savanna [*Hély et al.*, 2003], and 28–17,905 kW m^{-1} in woody savanna [*Govender et al.*, 2006]. The potential maximum fire intensity in the study area predicted by SPITFIRE is 3,800 to 13,000 kW m^{-1} for fire return intervals of 1–5 years.

Figure 2. Relationship between the mean fire return interval (years) and the mean fire intensity (kW m^{-1}) over 500 year simulations. Mean aboveground woody biomass (Mg C ha^{-1}) is shown by colors. Contours show the mean annual aboveground grass biomass (Mg C ha^{-1}). Red rectangle shows the limit of the fire return interval and fire intensity observed at an experimentally burnt miombo woodland.
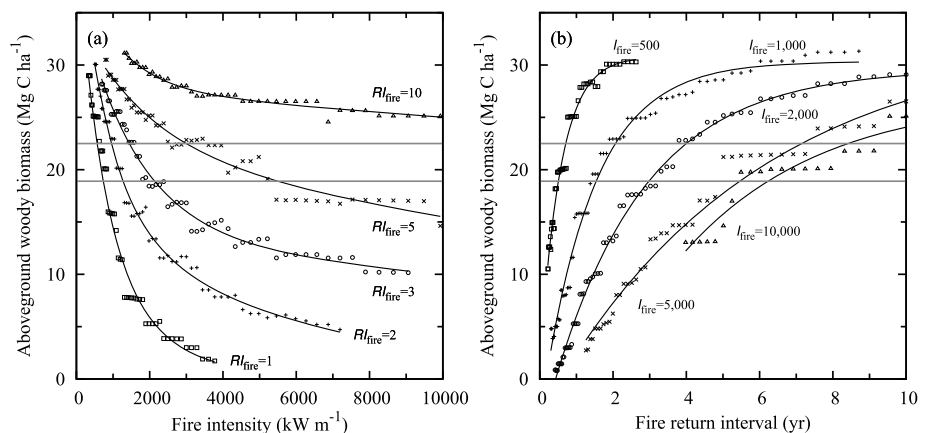
Figure 3. Effect of fire return interval (years) and fire intensity (kW m^{-1}) on aboveground woody biomass (Mg C ha^{-1}). (a) Relationship between aboveground woody biomass and fire intensity at fire return intervals of 1, 2, 3, 5, and 10 years. (b) Relationship between aboveground woody biomass and fire return interval at fire intensities of 500, 1000, 2000, 5000, and 10,000 kW m^{-1}. Solid curves are the fitted regressions, and gray solid lines show the mean aboveground woody biomass at the miombo woodlands site [*Woollen et al.*, 2012]. The biexponential model, $y = a \cdot \exp(-\exp(b) \cdot x) + c \cdot \exp(-\exp(d) \cdot x)$, was empirically fitted to the model output. It provided a good description of the relationship between I_{fire} and AGB for each RI_{fire} with $R^2 > 0.97$ (Figure 3a). The relationship between AGB and RI_{fire} is well described by the asymptotic regression model, $y = a \cdot (1 - \exp(-\exp(b) \cdot (x - c)))$, with $R^2 > 0.97$ for each I_{fire} (Figure 3b).

The mean predicted AGB (19.1 ± 7.6 Mg C ha^{-1}) agrees well with the observed mean AGB (20.7 ± 1.8 Mg C ha^{-1}). The minimum AGB in the model (1.7 Mg C ha^{-1}) is much lower than that observed (8.4 Mg C ha^{-1}), which might result from the assumption of spatially uniform fires in the grid, i.e., without fire-free space and thus with an excessively large impact. Another possible cause is that burnt miombo woodland might recover via lignotubers and root suckers rather than the establishment of seedlings, thereby becoming more fire resistant. The model might be unable to reproduce this rapid growth and adaptation to fire. The observed mean aboveground grass biomass was 1.5 ± 0.2 Mg ha^{-1} [*Woollen et al.*, 2012]. Under the observed fire disturbance, predicted mean aboveground grass biomass with eight different vegetation fractions was 1.1 ± 0.7 Mg C ha^{-1}.
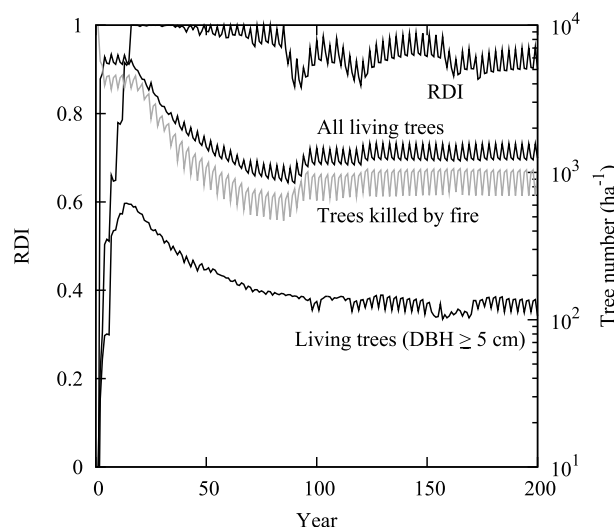

Figure 4. Variability in the relative density index (RDI) about the onset of self-thinning (Appendix: Equation (A4)) and the total number of living trees with DBH ≥ 5 cm (ha^{-1}), and trees killed by fire in the simulation with mean $I_{fire} = 1470$ kW m^{-1}, $RI_{fire} = 2$ year, and vegetation fraction of grass = 0.3.

Differences of AGB extracted from Figure 2 are shown in Figure 3 for some fire return intervals and fire intensities. Variation in AGB is more sensitive to changes in RI_{fire} with lower I_{fire}. A 1 year difference in RI_{fire} leads to large differences of up to 200% in AGB for $I_{fire} < 2000$ kW m^{-1}. This can be attributed to the effect of fire return interval on increasing small tree dominance [*Higgins et al.*, 2007]. The fire suppression period required for growth of the miombo woodland up to mean observed AGB increases with increasing I_{fire}.

Figure 4 shows an example of tree density dynamics in the case of mortality induced by both fire disturbance ($I_{fire} = 1470$ kW s^{-1} and $RI_{fire} = 2$ yr) and self-thinning. The number of trees with DBH ≥ 5 cm increases with years after stand-replacing fire, reaching 618 ha^{-1} after 14 years before declining. When
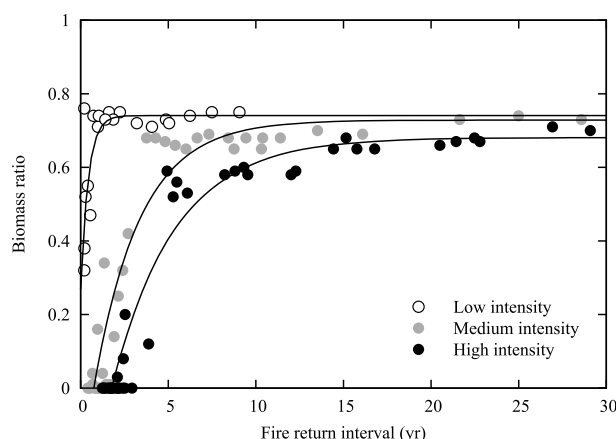
Figure 5. Relationship between the fire return interval (years) and the ratio of tree biomass with DBH ≥ 30 cm to total biomass. Fire intensity is divided into three groups: low, $I_{fire} \leq 1000$ kW m^{-1}; medium, $2000 \leq I_{fire} \leq 4000$ kW m^{-1}; and high, $I_{fire} > 5000$ kW m^{-1}. An asymptotic regression model is fitted to the data for each fire intensity group.

the relative density index (RDI) that describes self-thinning exceeds unity, tree density declines until RDI is less than unity (see Appendix A2). It appears that self-thinning occurs during the period 16–85 years after the stand-replacing fire. Self-thinning mortality, especially for juvenile trees, was found in almost all of the simulations, except for those with high living grass biomass and short fire return intervals. On average, the simulation shown in Figure 4 used 6% of total NPP in support of resprouting, but the carbon requirement ranged between 0.03% and 94% by fire regime over the ensemble of simulations.

Individual trees with DBH > 30 cm are categorized as large trees in miombo woodland [*Woollen et al.*, 2012]. In this study, we simply classified trees with a DBH ≤ 30 cm as being in their development phase and those > 30 cm as mature trees. There were clear differences ($P < 0.001$) in the biomass fraction of mature trees in the total AGB as a function of fire intensity and fire return interval (Figure 5). The maximum fraction of mature AGB varied between 0.68 and 0.74 among the fire intensity groups. Fire intensity has a statistically significant effect ($P < 0.001$) on the tree population structure of miombo woodland. In our simulation, fire return intervals of 2, 13, and 18 years were needed for the development of miombo woodland to a stable mature stage (99% of the maximum fractions) in the case of low, medium, and high fire intensity, respectively.

Frequent fires result in topkill of miombo woodland and suppress the growth of individuals toward their mature stage. This results in lower aboveground biomass (Figure 2) and means that juveniles resprouting after fire make a major contribution to the total biomass. An increase in the fire return interval allows individuals to accumulate biomass, helping them to survive subsequent fires, and thus increasing the proportion of mature trees in the total AGB.

Ryan and Williams [2011] constructed a gap-phase dynamic model based on fire experiments in miombo woodlands. The model estimates the sensitivity of tree populations and biomass to fire intensity and fire return interval. This gap model includes schemes to represent resprouting after fire and fire-induced and intrinsic mortality processes. Our predicted changes in BA and AGB under different fire intensities and fire return intervals appear to agree with their results at $RI_{fire} \leq 4$–5 yr. However, mean values of BA and AGB under long fire-free intervals ($RI_{fire} \geq 50$ yr), 12 m^2 ha^{-1} and 35 Mg C ha^{-1}, were lower than those of *Ryan and Williams* [2011] by at least ∼50%. The large difference between these studies is due, in part, to differences in mortality scheme under fire exclusion: this study used self-thinning mortality [*Sea and Hanan*, 2012], whereas *Ryan and Williams* [2011] employed a fixed mortality rate as intrinsic mortality [*Desanker and Prentice*, 1994]. This discrepancy cannot be resolved by the present study; however, the variations of tree populations and biomass under current fire regimes in miombo woodland are comparable to those from the gap model.

3.3. Fire Regimes Under Future Climate

The 11 different climate models considered here projects a change in temperature by 1.9 to 4.0°C and an average change in precipitation of −0.7 to +1.9 mm d^{-1} by 2100. Annual means of future climate variables estimated from the many available CMIP3 models show warmer and slightly increasing precipitation conditions in the study area. Predicted end-of-the-century changes from current climate in mean precipitation, specific humidity, and air temperature are +46 mm yr^{-1} (from 941 to 987 mm yr^{-1}), +2.3 g kg^{-1} (from 12.7 to 15.0 g kg^{-1}), and +3.3°C (from 24.1 to 27.4°C), respectively. However, there is little change in mean relative humidity (%) estimated from mean air temperature and specific humidity with atmospheric pressure of 1013.25 hPa, being −2% (from 68% to 66%). ORCHIDEE-FM-SPITFIRE was run by repeating the future climate
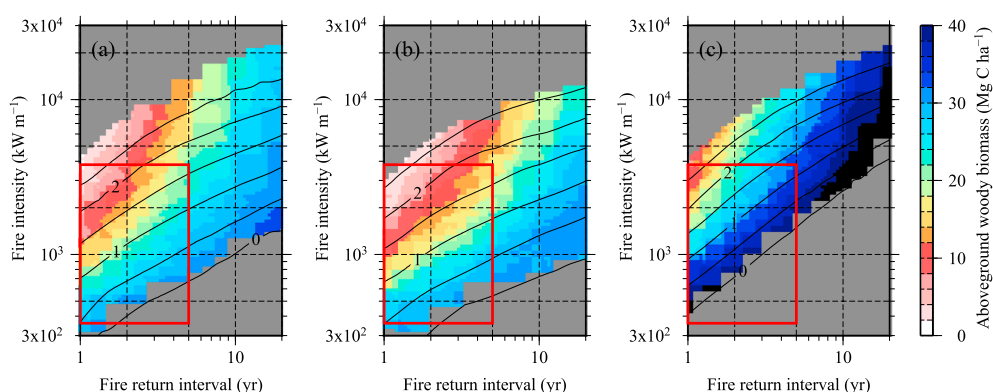
Figure 6. As in Figure 2 but for the simulations under three different conditions in (a) current climate and CO_2 concentration, (b) future climate and current CO_2 concentration, and (c) future climate and future CO_2 concentration. The black color in Figure 6c indicates an aboveground woody biomass of > 40 Mg C ha^{-1}. Red rectangles show the limit of the fire return interval and fire intensity observed at an experimentally burnt miombo woodland.

forcing with both current and future CO_2 concentrations, 380 ppm and 784 ppm, respectively, in the same manner as the simulation with the current climate. The simulations did not consider the influence of land cover change and the decadal-scale climate anomalies introduced by external climate oscillations, such as El Niño–Southern Oscillation.

The mean AGBs simulated under future climate conditions from an ensemble of fire regimes (see Appendix B) and with different CO_2 concentrations are shown in Figures 6b and 6c. Predicted AGB is significantly correlated with the fire return intervals and fire intensity ($P < 0.001$) under future climate conditions, regardless of CO_2 concentration. With the same fire regimes as the experimentally burnt miombo woodland, significant changes in AGB are predicted ($P < 0.001$) in response to changes in climate conditions and CO_2 concentrations when compared with AGB under the current climate (Figure 6a), i.e., a mean AGB of 17.5 ± 8.1 Mg C ha^{-1} (91% of present AGB) for future climate with the current CO_2 concentration (Figure 6b) and 29.1 ± 7.5 Mg C ha^{-1} (152% of the present AGB) for future climate and CO_2 concentration (Figure 6c). Applying Student's t test to the results shown in Figure 6 (i.e., simulations with three different combinations of climate and CO_2 concentration), the effect of changes in climate and CO_2 concentration on AGB are significant ($P < 0.001$) over all fire regimes. Under the future climate with the current CO_2 concentration, gross primary product (GPP) decreased due to a decline in the rate of net CO_2 assimilation limited by the ribulose 1.5 bisphosphate carboxylase/oxgenase. A gradual drop in the rate of CO_2 assimilation was found from about 18–20°C. Consequently, NPP and AGB also decreased, which resulted in a subsequent decrease of the deadwood fuel pool (Table 2). Under the future climate and CO_2 concentration, NPP significantly increases, leading to increased AGB. However, increasing AGB also increases the wood fuel, which may slightly enhance the fire intensity. Furthermore, fire intensity and its range also changed due to variations in living grass biomass associated with climate and CO_2 concentration. This negative retroaction through fire can thus limit the increase of AGB. These results suggest that a warmer climate with elevated atmospheric CO_2 concentrations can mitigate the effect of fire disturbance on AGB in miombo woodland, while it is highly vulnerable to fire if climate change is the only driver. The minor effect of fire on AGB allows miombo woodlands to sustain their current AGB with a fire return interval of 1 or 2 years if fire intensity is

Table 2. Simulated Carbon Fluxes and Pools Using Climate Conditions for the Study Area for 2006–2008 and 2091–2100 and CO_2 Concentrations of 380 and 784 ppm Without Fire Disturbance[a]

Climate	CO_2	GPP	AR	NPP	$DF_{1 h}$	$DF_{10 h}$	$DF_{100 h}$	$DF_{1000 h}$
2006–2008	380	13.9	7.0	6.8	5.5	0.5	0.8	9.5
2091–2100	380	10.4	5.0	5.4	3.6	0.3	0.5	6.2
2091–2100	784	23.0	11.3	11.8	9.5	1.0	1.6	19.6

[a]The tabulated fluxes are annual mean gross primary product (GPP), autotrophic respiration (AR), and NPP (Mg C ha^{-1} yr^{-1}). The pool is the mean deadwood fuel mass (DF) in 1, 10, 100, and 1000 h time lag classes (Mg C ha^{-1}).

constrained to be lower than 1500 and 4500 kW m^{-1}, respectively. For $RI_{fire} > 3$ yr, miombo woodlands are predicted to increase their AGB above the current value regardless of fire intensity.

4. Discussion

4.1. Fire Management

Ryan and Williams [2011] observed that when a potential miombo woodland site in Zimbabwe was subjected to over 50 years of annual burning, no woody plant survived; under this regime the miombo woodland becomes a grass-dominated landscape [*Furley et al.*, 2008]. The current study, based on a triad of models (ORCHIDEE-FM-SPITFIRE) calibrated with in situ observations, found similar results with woody AGB cover being close to zero in the presence of abundant living grass biomass, leading to a high fire intensity (Figure 2). However, trees were able to survive, and their biomass increased with decreasing living grass biomass and fire intensity, even for annually returning fires. These findings are consistent with previous studies in a savanna in tropical Australia [*Andersen*, 1991], and in African savannas in Kruger National Park [*Higgins et al.*, 2007] and Burkina Faso [*Traoré et al.*, 2008]. In these studies, trees were reported to survive under prescribed annual fire experiments, although repeated fires kept tree size small. Our results suggest that live grass biomass exerts a negative feedback on woody AGB in fire-disturbed savannas due to a positive relationship between grass biomass and fire intensity. Indeed, direct or indirect changes in grass biomass (e.g., by a change in grazing or browsing intensity) result in changes in fire intensity and fire return interval and subsequent changes in the tree/grass ratio. In turn, this can lead to switching from savanna to forest or grassland [*Van Langevelde et al.*, 2003]. Our model is unable to explain continuous changes in vegetation structure or the tree-to-grass ratio and their effect on variations in fire intensity because we prescribed tree/grass ratios for each simulation. Our discrete simulations, however, indicate that suppressing the development of a grass layer and grass invasion decreases fire intensity and prevents the biomass of woody vegetation from diminishing, and vice versa.

Fire intensity varies with the season and is driven mainly by the moisture content of the grass biomass. That is, the highest fire intensity occurs late in the dry season and the lowest fire intensity in the wet season [*Govender et al.*, 2006]. Fires in the dry season have been reported to reduce the woody biomass more than fires during the wet season [*Smit et al.*, 2010]. These results prompt speculation that the amount of flammable grass biomass controls the fire regime in savanna, in a similar way to the size of the deadwood pools because both biomass pools provide fuel to the fire [*Trollope et al.*, 1996].

Fire occurs at least every 2 years in approximately half of the total burned area in Africa [*Barbosa et al.*, 1999]. In miombo woodland, the mean fire return interval is estimated to range between 1.6 and 3 years [*Frost*, 1996]. Our model predicts that under such a fire return interval, miombo woodlands can sustain their current woody AGB if fire intensities remain below 930–1700 kW m^{-1}. Fires with such intensities are, in general, observed during the early dry season in miombo woodland [*Hoffa et al.*, 1999] and in savanna [*Gambiza et al.*, 2005]. In fact, there are no significant differences in the distribution of tree diameter in miombo woodland under fire protection regimes and early burning regimes [*Chidumayo*, 1988]. By the middle of the dry season, however, the fire intensity typically exceeds 5000 kW m^{-1} due to the lower moisture content of the grass biomass [*Hoffa et al.*, 1999]. Natural fires caused by lightning occur during thunderstorms at the end of the dry season [*Bloesch*, 1999]. Although human-induced fires can occur all year round, they are mostly in the late dry season because local communities find this time best for clearing bush, fertilizing arable fields, and killing diseases and pests [*Eriksen*, 2007]. However, this study suggests that frequent fire in the late dry season will induce more intense fire and consequently encourage the development of a grass layer, which will result in further, more intense fires and consequent degradation of the woody biomass. In many cases, fire suppression policies have failed and resulted in increasing rather than decreasing numbers of damaging fires late in the dry season [*Laris and Wardell*, 2006]. Therefore, a consensus on fire treatment by local communities, such as the use of low-intensity prescribed fire in the early dry season, or mowing and grazing of the grasses, would be useful to preserve woodland and sustain the benefits it provides. For instance, seasonal mosaic burning reduces fire damage in the late dry season and thus may be an effective fire management strategy [*Laris*, 2002; *Laris and Wardell*, 2006].

4.2. Effect of Fire on Vegetation Structure

The model predicted that when fire becomes less frequent or less intense, woody vegetation will increase its aboveground biomass and that the vegetation structure will shift toward a denser savanna, leading to
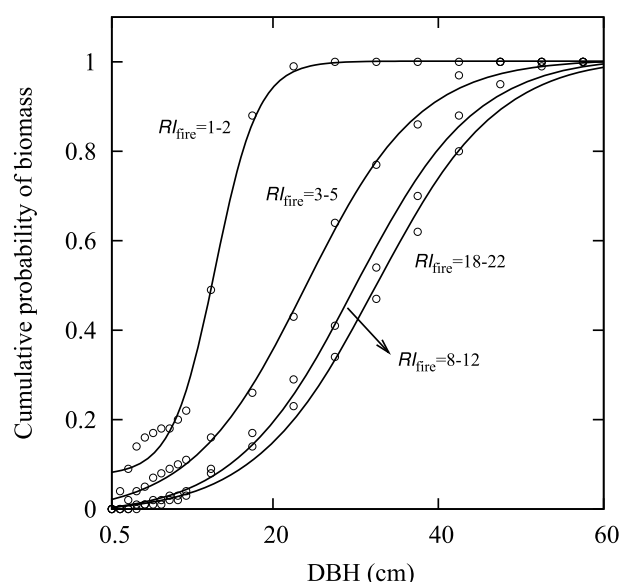
Figure 7. Cumulative probability distribution functions of total woody biomass against DBH (cm), with four different groups of fire return interval (years) under conditions with high fire intensity ($\geq 5\,000$ kW m^{-1}).

less frequent fires (Figures 2 and 3). Long fire-free intervals induce a gradual but progressive increase in the density of the woody vegetation, leading to high-biomass but low-density woodlands with more mature trees (Figure 7). As woody vegetation increases, grass production declines dramatically, which further reduces the fire frequency [*Scholes and Archer*, 1997]. Additionally, fire exclusion enables the establishment of fire-sensitive species, which can lead to the appearance of a more wooded physiognomy [*Moreira*, 2000] and a succession from savanna to forest. Our model, however, does not account for temporal changes in dominant woody species and living grass cover or the succession from savanna to forest. These shortcomings in the model could contribute to the difference between observed and simulated woody production under long fire-free intervals. Hence, further model developments are required to assess the dynamics of woody vegetation and grass in response to fire regimes and climate [e.g., *Scheiter and Higgins*, 2009].

If fire occurs in miombo woodland, almost all woody plants survive, but if the fire intensity is sufficiently high, a substantial number of trees are topkilled. Miombo woodland, however, can recover from topkill by resprouting from the rootstocks that survived the fire [*Ryan and Williams*, 2011]. The topkill rate for a fire varies with tree size, with smaller trees being more susceptible than larger trees (Appendix: Figure A1). With frequent burning, trees can be trapped into topkill more often, thereby preventing individuals from reaching maturity, thus reducing the biomass of the population (Figures 2 and 7).

As shown in Figure A1 in the Appendix, fire intensity controls the severity of topkill in individual size classes. *Williams et al.* [2009] reported that in a tropical savanna in northern Australia, the amount of topkilled stems created by a single fire of 20,000 kW m^{-1} was comparable to that of an annual burn for 5 years with an average intensity of 8000 kW m^{-1}. For intense fires, trees in the large size class are more likely to be topkilled, leading to a large biomass loss in the ecosystem and requiring a long period to restore it to preburn size and biomass. After a topkill, the resprouted trees are exposed to more severe pressure of subsequent topkill due to the reduction in tree size [*Hoffmanna and Solbrig*, 2003]. Therefore, intense fires act as a demographic bottleneck on the route to tree maturity. Furthermore, topkill results in a more open canopy structure which allows grasses to invade forest [*Scheiter et al.*, 2012] and dries the understory, leading to suitable conditions for rapid encroachment of flammable grasses, in turn enhancing the risk of fire occurrence and increasing its intensity [*Bond*, 2001].

4.3. Miombo Woodland in Future Climate

A future climate that is warmer with slightly higher precipitation compared with today's climate, and with elevated CO_2, led to an increase in the modeled mean miombo woodland AGB of about 52% compared with the current climate and today's fire regime. Enhanced growth of miombo woodland under a future climate is consistent with the general behavior of woody plants that use the C3 carbon fixation metabolic pathway. The elevated CO_2 promotes the regrowth of juveniles after fire and relieves woody plants from fire disturbance due to changes in the fire regime [*Bond and Midgley*, 2000]. Increases in woody cover and density have been observed in mesic savanna under elevated CO_2 and warming conditions [*Buitenwerf et al.*, 2012; *Volder et al.*, 2013], which favor C3 photosynthesis relative to C4. Climate change alone, however, caused a 9% decrease in mean aboveground woody biomass in our simulation. At the current CO_2 level, increasing temperature results in a more frequent exceedance of the photosynthetic thermal optimum, leading to a decline in the net CO_2 assimilation rate. In our model, optimum photosynthesis temperatures
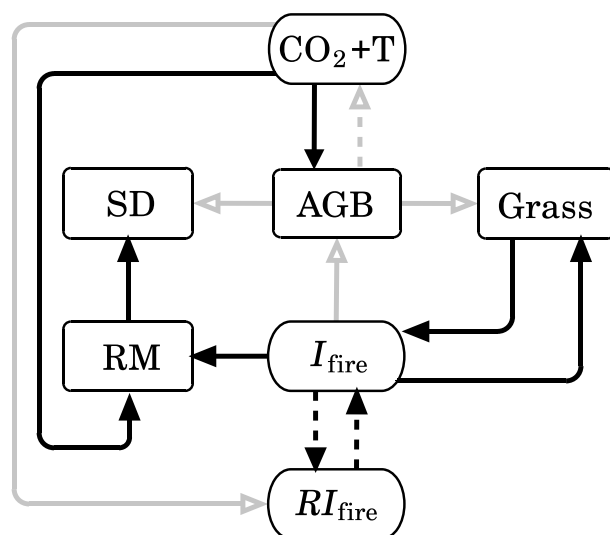
Figure 8. Interaction loops between and among aboveground woody biomass (AGB), stocking density (SD), recruitment of juveniles after fire (RM), and grass biomass (Grass) in miombo woodland, and fire intensity (I_{fire}), fire return interval (RI_{fire}), and warming climate with elevated atmospheric CO_2 (CO_2+T). The positive effects are connected by black lines with closed arrows; negative effects are shown by gray lines with open arrows. Broken lines indicate effects not simulated in this study does not simulate.

are prescribed to 37 and 36°C for C3 trees and C4 grasses [*Krinner et al.*, 2005], respectively. However, the net CO_2 assimilation rate for C3 trees shows a peak at approximately 20°C but declines above 30°C due to limitations of water and CO_2 concentration. Similar temperature responses have been observed in an African savanna where the net CO_2 assimilation rate declines gradually at temperatures above 25°C [*Franklin et al.*, 2004]. When using mean changes in relative humidity as simple sensitivity tests of water stress on net CO_2 assimilation, it was observed that a slight change in water stress under a future climate had little effect on the net CO_2 assimilation. Furthermore, savanna woody species with well-developed drought tolerance can survive and increase their aboveground woody biomass even under the warming condition with severe summer water limitation [*Volder et al.*, 2013].

Conversely, C4 grass species in savanna are expected to be suppressed and largely replaced by competing C3 species with greater stimulation of C3 photosynthetic efficiency, under high CO_2 concentrations and warming [*Collatz et al.*, 1998; *Higgins and Scheiter*, 2012]. This decline in C4 grasses and reduction in transpiration rate from grass associated with lowered stomatal conductance by elevated CO_2 slows the depletion of soil water by grasses, allowing increasing percolation and resulting in higher water availability for woody plants [*Polley et al.*, 1997]. This supports our result that a future climate with elevated CO_2 has a significant positive effect on woody plant growth in miombo woodland, which is likely to result in a decrease in the fire frequency and intensity that in turn enhances the growth of woody biomass.

Aboveground woody biomass in miombo woodland is fundamentally linked with fire regime, climate change with elevated atmospheric CO_2, and grass biomass (Figure 8). The realized aboveground woody biomass is the outcome of processes that are commonly counteracting. A lengthened fire return interval will build up the fuel load, thereby promoting high-intensity fires due to the accumulation of dead fuel. High-intensity fires can reduce the risk of high-frequency burning with high intensity by removing dead fuel. Consequently, high-intensity low-frequency burning is expected to result in conditions that are unfavorable for low-intensity, high-frequency fires. In addition, high-intensity fires decrease the aboveground woody biomass and accumulated dead fuel, thereby stimulating the recruitment of juveniles through resprouting. This leads to a high tree density with young and small trees. At the same time, high-intensity fires allow the encroachment of grasses in the burnt open canopy. Grass biomass has a strong effect on fire risk and intensity. Increasing aboveground biomass (potentially through elevated CO_2 and increased temperature) enhances terrestrial carbon uptake from the atmosphere. Conversely, replacement of miombo woodland by grassland will partly offset carbon uptake by deforestation. Loss of woodland may result in attenuation of the regional hydrological cycle (i.e., less evapotranspiration and cloud formation) and a reduction in regional precipitation, which leads to a longer dry season and could, in turn, enhance fires [*Beerling and Osborne*, 2006]. As another indirect effect, soot released by enhanced fires causes further warming [*Menon et al.*, 2002], thus facilitating the expansion of grassland and therefore leading to more fires.

4.4. Limitations
Key limitations in this study are the model's prescribed vegetation fraction between grass and woody plants, the static parametrization of the interactions between CO_2 and nutrients, and the uncertainty in the climate predictions, as explained below.

1. The model's prescribed vegetation fraction between grass and woody plants does not simulate changes in tree/grass cover by fire regimes and thus neglects the interaction between trees and grass and its feedback on fire regime.

2. As suggested by experiments in Cerrado savanna in Brazil [*Hoffmann et al.*, 2000], the effects of enhanced atmospheric CO_2 concentration on the growth of savanna will be limited if the savanna is nutrient limited, which is the case for miombo woodland [*Campbell*, 1996]. The version of ORCHIDEE used in this study accounts for the interactions between CO_2 and nutrients through its parametrization of photosynthesis. This approach is acceptable for present-day simulations but falls short in quantifying the interactions between CO_2 and nutrients under changing environmental conditions. Consequently, our simulations may overestimate the effect of CO_2 fertilization on biomass growth in miombo woodland.

3. Uncertainty in future climate predictions, especially over Africa, propagates into our simulations. Improving the representation of future climate, including future climate changes in all forcing variables and altering rainfall frequency and intensity, would improve the model relationship between miombo woodland and fire regime under a future climate.

   Given that ORCHIDEE is designed and used as a large-scale model, it does not account for several small-scale processes that may be important, especially at the local scale, as follows.

4. Changes in tree species composition of miombo woodland are unaccounted for. It is likely that future environmental conditions will favor species with a higher nutrient efficiency than today's dominant species. If this is the case, our simulations could underestimate future biomass growth of miombo woodland.

5. The model also neglects the action of termites. Because termites consume litter in savanna, especially during the dry season [*Ohiagu and Wood*, 1979], they may have an impact on the fire regime by removing flammable dead fuel.

6. The fate of miombo woodland is strongly dependent on human factors, especially population growth that will control, for example, the frequency of fire, grazing intensity, and wood harvest. As demonstrated in this study, changes in fire frequency and fire intensity could offset, in either direction, the effects of climate changes.

7. Wind speed has a positive feedback on fire intensity [*Beer*, 1991] and thus consequently tree mortality [*Ansley et al.*, 1998]. Clearance of woodlands enhances wind speed [*Kainkwa and Stigter*, 1994] and therefore indirectly results in more intense fire [*Hoffmann et al.*, 2002]. The biophysical effects of fire frequency and its intensity on savanna woodlands remain largely unknown [*Göergen et al.*, 2006].

5. Conclusions

Fire has a large impact on aboveground woody biomass and vegetation structure in miombo woodland. Fire retards the development of trees to maturity by removing aerial biomass and reducing tree size. The severity of fire disturbance to woody plants varies significantly with the fire regime, i.e., with fire return interval and fire intensity. A shorter fire return interval and higher fire intensity results in a greater reduction of aboveground woody biomass by reducing the mean tree size within the population. Fires in miombo woodland are mostly human induced, and the fire return interval is effectively a management tool. However, fire intensity depends on the amount of grass fuel available for combustion and on the season. The current practice of frequent burning needs to be replaced with more rigorous fire control if today's miombo woodland ecosystem is to be sustained. Available data suggest that elevated CO_2 concentrations, warming, and slightly increasing precipitation in the future would increase plant production, perhaps allowing an increase in the resprouting capacity and growth rate of woody plants and thus resulting in miombo woodland becoming more fire resistance.

Appendix

The supplement file describes the model used here.

References

Abbot, J. I. O., and K. Homewood (1999), A history of change: Causes of miombo woodland decline in a protected area in Malawi, *J. Appl. Ecol.*, *36*, 422–433.

Andersen, A. N. (1991), Responses of ground-foraging ant communities to three experimental fire regimes in a savanna forest of tropical Australia, *Biotropica*, *23*, 575–585.

Ansley, R. J., D. L. Jones, T. R. Tunnell, B. A. Kramp, and P. W. J. PW (1998), Honey mesquite canopy responses to single winter fires: Relation to herbaceous fuel, weather and fire temperature, *Int. J. Wildland Fire*, *8*, 241–252.

Archibald, S., D. P. Roy, B. W. Van Wilgen, and R. J. Scholes (2009), What limits fire? An examination of drivers of burnt area in Southern Africa, *Global Change Biol.*, *15*, 613–630.

Barbosa, P. M., D. Stroppiana, J. Grégoire, and J. M. Cardoso Pereira (1999), An assessment of vegetation fire in Africa (1981–1991): Burned areas, burned biomass, and atmospheric emissions, *Global Biogeochem. Cycles*, *13*, 933–950.

Beer, T. (1991), The interaction of wind and fire, *Boundary Layer Meteorol.*, *54*, 287–308.

Beerling, D. J., and C. P. Osborne (2006), The origin of the savanna biome, *Global Change Biol.*, *12*, 2023–2031.

Bellassen, V., G. le Maire, J. F. Dhôte, P. Ciais, and N. Viovy (2010), Modelling forest management within a global vegetation model—Part 1: Model structure and general behaviour, *Ecol. Modell.*, *221*, 2458–2474.

Berjak, S. G., and J. W. Hearne (2002), An improved cellular automaton model for simulating fire in a spatially heterogeneous Savanna system, *Ecol. Modell.*, *148*, 133–151.

Bloesch, U. (1999), Fire as a tool in the management of a savanna/dry forest reserve in Madagascar, *Appl. Vegetation Sci.*, *2*, 117–124.

Bond, W. (2001), Ecological effects of fires, *Encyclop. Biodiv.*, *2*, 745–753.

Bond, W., and G. Midgley (2000), A proposed CO_2-controlled mechanism of woody plant invasion in grasslands and savannas, *Global Change Biol.*, *6*, 865–869.

Bond, W. J., F. I. Woodward, and G. F. Midgley (2005), The global distribution of ecosystems in a world without fire, *New Phytol.*, *165*, 525–538.

Buitenwerf, R., W. J. Bond, N. Stevens, and W. S. W. Trollope (2012), Increased tree densities in south african savannas: > 50 years of data suggests CO_2 as a driver, *Global Change Biol.*, *18*, 675–684.

Campbell, B. (1996), *The Miombo in Transition: Woodlands and Welfare in Africa*, 266 pp., Center For International Forestry Research, Bogor, Indonesia.

Chidumayo, E. N. (1988), A re-assessment of effects of fire on miombo regeneration in the Zambian Copperbelt, *J. Tropical Ecol.*, *4*, 361–372.

Ciais, P., A. Bombelli, M. Williams, S. L. Piao, J. Chave, C. M. Ryan, M. Henry, P. Brender, and R. Valentini (2011), The carbon balance of Africa: Synthesis of recent research studies, *Phil. Trans. R. Soc*, *369*, 2038–2057.

Clark, T. L., J. Coen, and D. Latham (2004), Description of a coupled atmosphere-fire model, *Int. J. Wildland Fire*, *13*, 49–63.

Collatz, G. J., J. A. Berry, and J. S. Clark (1998), Effects of climate and atmospheric CO_2 partial pressure on the global distribution of C_4 grasses: Present, past, and future, *Oecologia*, *114*, 441–454.

Dee, D. P., et al. (2011), The ERA-Interim reanalysis: Configuration and performance of the data assimilation system, *Q. J. R. Meteorol. Soc.*, *137*, 553–597.

Desanker, P. V., and I. C. Prentice (1994), MIOMBO—A vegetation dynamics model for the miombo woodlands on Zambezian Africa, *For. Ecol. Manage.*, *69*, 87–95.

Dhôte, J.-F., and J.-C. Hervé (2000), Changements de productivité dans quatre forêts de chênes sessiles depuis 1930: Une approche au niveau du peuplement, *Ann. For. Sci.*, *57*, 651–680.

D'Odorico, P., F. Laio, and L. Ridolfi (2006), A probabilistic analysis of fire-induced tree-grass coexistence in savannas, *Am. Nat.*, *167*, E79–E87.

Eriksen, C. (2007), Why do they burn the bush? Fire, rural livelihoods, and conservation in Zambia, *Geogr. J.*, *173*, 242–256.

Favier, C., J. Chave, A. Fabing, D. Schwartz, and M. A. Dubois (2004), Modelling forest-savanna mosaic dynamics in man-influenced environments: Effects of fire, climate and soil heterogeneity, *Ecol. Modell.*, *171*, 85–102.

Fisher, B. (2010), African exception to drivers of deforestation, *Nat. Geosci.*, *3*, 375–376.

Franklin, M. G., J. N. Aranibar, K. B. Mantlana, and S. Macko (2004), Photosynthetic and gas exchange characteristics of dominant woody plants on a moisture gradient in an African savanna, *Global Change Biol.*, *10*, 309–317.

Frost, P. G. H. (1996), The ecology of miombo woodlands, in *The Miombo in Transition: Woodlands and Welfare in Africa*, edited by B. M. Campbell, pp. 11–55, Center for International Forestry Research, Bogor, Indonesia.

Frost, P. G. H. (1999), Fire in Southern African woodlands: Origins, impacts, effects and control, in *Proceedings of an FAO Meeting on Public Policies Affecting Forest Fires, FAO Forestry Paper 138*, pp. 181–205, Food and Agriculture Organization of the United Nations, Rome, Italy.

Furley, P. A., R. M. Rees, C. M. Ryan, and G. Saiz (2008), Savanna burning and the assessment of long-term fire experiments with particular reference to Zimbabwe, *Prog. Phys. Geogr.*, *32*, 611–634.

Gambiza, J., B. Campbell, S. R. Moe, and P. G. H. Frost (2005), Fire behaviour in a semi-arid Baikiaea plurijuga savanna woodland on Kalahari sands in western Zimbabwe, *S. Afr. J. Sci.*, *101*, 239–244.

Göergen, K., A. H. Lynch, A. G. Marshall, and J. Beringer (2006), Impact of abrupt land cover changes by savanna fire on northern Australian climate, *J. Geophys. Res.*, *111*, D19106, doi:10.1029/2005JD006860.

Govender, N., W. S. W. Trollope, and B. W. Van Wilgen (2006), The effect of fire season, fire frequency, rainfall and management on fire intensity in savanna vegetation in South Africa, *J. Appl. Ecol.*, *43*, 748–758.

Hély, C., S. Alleaume, R. J. Swap, H. H. Shugart, and C. O. Justice (2003), SAFARI-2000 characterization of fuels, fire behavior, combustion completeness, and emissions from experimental burns in infertile grass savannas in western Zambia, *J. Arid. Environ.*, *54*, 381–394.

Higgins, S. I., and S. Scheiter (2012), Atmospheric CO_2 forces abrupt vegetation shifts locally, but not globally, *Nature*, *488*, 209–212.

Higgins, S. I., W. J. Bond, and W. S. W. Trollope (2000), Fire, resprouting and variability: A recipe for grass-tree coexistence in savanna, *J. Ecol.*, *88*, 213–229.

Higgins, S. I., et al. (2007), Effects of four decades of fire manipulation on woody vegetation structure in savanna, *Ecology*, *88*, 1119–1125.

Hoffa, E. A., D. E. Ward, W. M. Hao, R. A. Susott, and R. H. Wakimoto (1999), Seasonality of carbon emissions from biomass burning in a Zambian savanna, *J. Geophys. Res.*, *104*, 13,841–13,853.

Hoffmann, W. A. (1999), Fire and population dynamics of woody plants in a neotropical savanna: Matrix model projections, *Ecology*, *80*, 1354–1369.

Hoffmann, W., F. Bazzaz, N. Chatterton, P. Harrison, and R. Jackson (2000), Elevated CO_2 enhances resprouting of a tropical savanna tree, *Oecologia*, *123*, 312–317.

Hoffmann, W. A., W. Schroeder, and R. B. Jackson (2002), Positive feedbacks of fire, climate, and vegetation and the conversion of tropical savanna, *Geophys. Res. Lett.*, *29*, 2052, doi:10.1029/2002GL015424.

Hoffmanna, W. A., and O. T. Solbrig (2003), The role of topkill in the differential response of savanna woody species to fire, *For. Ecol. Manage.*, *180*, 273–286.

Kainkwa, R. M. R., and C. J. Stigter (1994), Wind reduction downwind from a savanna woodland edge, *Neth. J. Agric. Sci.*, *42*, 145–157.

Krinner, G., N. Viovy, N. de Noblet–Ducoudré, J. Ogée, J. Polcher, P. Friedlingstein, P. Ciais, S. Sitch, and I. C. Prentice (2005), A dynamic global vegetation model for studies of the coupled atmosphere-biosphere system, *Global Biogeochem. Cycles*, *19*, GB1015, doi:10.1029/2003GB002199.

Lambin, E. F., H. J. Geist, and E. Lepers (2003), Dynamics of land-use and land-cover change in tropical regions, *Annu. Rev. Environ. Resour.*, *28*, 205–241.

Laris, P. (2002), Burning the seasonal mosaic: Preventative burning strategies in the wooded savanna of southern Mali, *Hum. Ecol.*, *30*, 155–186.

Laris, P., and D. A. Wardell (2006), Good, bad or 'necessary evil'? Reinterpreting the colonial burning experiments in the savanna landscapes of West Africa, *Geog. J.*, *172*, 271–290.

Leriche, H., X. Le Roux, J. Gignoux, A. Tuzet, H. Fritz, L. Abbadie, and M. Loreau (2001), Which functional processes control the short-term effect of grazing on net primary production in grasslands?, *Oecologia*, *129*, 114–124.

Liedloff, A. C., and G. D. Cook (2007), Modelling the effects of rainfall variability and fire on tree populations in an Australian tropical savanna with the FLAMES simulation model, *Ecol. Modell.*, *201*, 269–282.

Loveland, T. R., B. C. Reed, J. F. Brown, D. O. Ohlen, Z. Zhu, L. Yang, and J. W. Merchant (2000), Development of a global land cover characteristics database and IGBP DISCover from 1 km AVHRR data, *Int. J. Remote Sens.*, *21*, 1303–1330.

Mayer, A. L., and A. H. Khalyani (2011), Grass trumps trees with fire, *Science*, *334*, 188–189.

Mbow, C., K. Goïta, and G. B. Bénié (2004), Spectral indices and fire behavior simulation for fire risk assessment in savanna ecosystems, *Remote Sens. Environ.*, *91*, 1–13.

Meehl, G. A., C. Covey, T. Delworth, M. Latif, B. McAvaney, J. F. B. Mitchell, R. J. Stouffer, and K. E. Taylor (2007), The WCRP CMIP3 multi-model dataset: A new era in climate change research, *Bull. Am. Meteorol. Soc.*, *88*, 1383–1394.

Menon, S., J. Hansen, L. Nazarenko, and Y. Luo (2002), Climate effects of black carbon aerosols in China and India, *Science*, *297*, 2250–2253.

Moreira, A. G. (2000), Effects of fire protection on savanna structure in Central Brazil, *J. Biogeogr.*, *27*, 1021–1029.

Mouillot, F., and C. B. Field (2005), Fire history and the global carbon budget: A 1° × 1° fire history reconstruction for the 20th century, *Global Change Biol.*, *11*, 398–420, doi:10.1111/j.1365-2486.2005.00920.x.

Nesterov, V. G. (1949), *Gorimost'lesa i metody eio opredelenia*, Goslesbumaga, Moscow.

Ohiagu, C. E., and T. G. Wood (1979), Grass production and decomposition in Southern Guinea savanna, Nigeria, *Oecologia*, *40*, 155–165.

Peterson, D. W., and P. B. Reich (2001), Prescribed fire in oak savanna: Fire frequency effects on stand structure and dynamics, *Ecol. Appl.*, *11*, 914–927.

Pitman, A., G. Narisma, and J. McAneney (2007), The impact of climate change on the risk of forest and grassland fires in Australia, *Clim. Change*, *84*, 383–401.

Polley, H., H. Mayeux, H. Johnson, and C. Tischler (1997), Viewpoint: Atmospheric CO_2, soil water, and shrub/grass ratios on rangelands, *J. Range Manage.*, *50*, 278–284.

Poulter, B., L. Aragao, U. Heyder, M. Gumpenberger, J. Heinke, F. Langerwisch, A. Rammig, K. Thonicke, and W. Cramer (2010), Net biome production of the Amazon Basin in the 21st century, *Global Change Biol.*, *16*, 2062–2075.

Rothermel, R. C. (1972), A mathematical model for predicting fire spread in wildland fuels, *Research Paper INT-RP-115*, 40 pp., USDA Forests Service Research Paper, Ogden, UT.

Roy, D., L. Boschetti, C. Justice, and J. Ju (2008), The collection 5 MODIS burned area product—Global evaluation by comparison with the MODIS active fire product, *Remote Sens. Environ.*, *112*, 3690–3707.

Ryan, C. M., and M. Williams (2011), How does fire intensity and frequency affect miombo woodland tree populations and biomass?, *Ecol. Appl.*, *21*, 48–60.

Ryan, C. M., T. Hill, E. Woollen, C. Ghee, E. Mitchard, G. Cassells, J. Grace, I. H. Woodhouse, and M. Williams (2012), Quantifying small-scale deforestation and forest degradation in African woodlands using radar imagery, *Global Change Biol.*, *18*, 243–257.

Sala, O. E., et al. (2000), Global biodiversity scenarios for the year 2100, *Science*, *287*, 1770–1774.

Sankaran, M., et al. (2005), Determinants of woody cover in African savannas, *Nature*, *438*, 846–849.

Scheffer, M., S. Carpenter, J. A. Foley, C. Folke, and B. Walker (2001), Catastrophic shifts in ecosystems, *Nature*, *413*, 591–596.

Scheiter, S., and S. I. Higgins (2009), Impacts of climate change on the vegetation of Africa: An adaptive dynamic vegetation modelling approach, *Global Change Biol.*, *15*, 2224–2246.

Scheiter, S., S. I. Higgins, C. P. Osborne, C. Bradshaw, D. Lunt, B. S. Ripley, L. L. Taylor, and D. J. Beerling (2012), Fire and fire-adapted vegetation promoted C_4 expansion in the late Miocene, *New Phytologist*, *195*, 653–666.

Scholes, R. J., and S. R. Archer (1997), Tree-grass interactions in savannas, *Annu. Rev. Ecol. Syst.*, *28*, 517–544.

Sea, W. B., and N. P. Hanan (2012), Self-thinning and tree competition in savannas, *Biotropica*, *44*, 189–196.

Silva, J. F., J. Raventos, H. Caswell, and M. C. Trevisan (1991), Population responses to fire in a tropical savanna grass, Andropogon semiberbis: A matrix model approach, *J. Ecol.*, 345–355.

Simioni, G., X. Le Roux, J. Gignoux, and H. Sinoquet (2000), Treegrass: A 3D, process-based model for simulating plant interactions in tree–grass ecosystems, *Ecol. Modell.*, *131*, 47–63.

Smit, I. P. J., G. P. Asner, N. Govender, T. K. Bowdoin, D. E. Knapp, and J. Jacobson (2010), Effects of fire on woody vegetation structure in African savanna, *Ecol. Appl.*, *20*, 1865–1875.

Staver, A. C., S. Archibald, and S. A. Levin (2011), The global extent and determinants of savanna and forest as alternative biome states, *Science*, *334*, 230–232.

Thonicke, K., A. Spessa, I. C. Prentice, S. P. Harrison, L. Dong, and C. Carmona-Moreno (2010), The influence of vegetation, fire spread and fire behaviour on biomass burning and trace gas emissions: Results from a process-based model, *Biogeosciences*, *7*, 1991–2011.

Traoré, S., R. Nygård, S. Guinko, and M. Lepage (2008), Impact of macrotermes termitaria as a source of heterogeneity on tree diversity and structure in a Sudanian savannah under controlled grazing and annual prescribed fire (Burkina Faso), *For. Ecol. Manage.*, *255*, 2337–2346.

Trollope, W. S. W., L. A. Trollope, A. L. F. Potgieter, and N. Zambatis (1996), SAFARI-92 characterization of biomass and fire behavior in the small experimental burns in the Kruger National Park, *J. Geophys. Res.*, *101*, 23,531–23,539.

Van der Werf, G. R., J. T. Randerson, G. J. Collatz, and L. Giglio (2003), Carbon emissions from fires in tropical and subtropical ecosystems, *Global Change Biol.*, *9*, 547–562.

Van Langevelde, F., et al. (2003), Effects of fire and herbivory on the stability of savanna ecosystems, *Ecology*, *84*, 337–350.

Volder, A., D. Briske, and M. Tjoelker (2013), Climate warming and precipitation redistribution modify tree-grass interactions and tree species establishment in a warm-temperate savanna, *Global Change Biol.*, *19*, 843–857.

Williams, A. A. J., D. J. Karoly, and N. Tapper (2001), The sensitivity of Australian fire danger to climate change, *Clim. Change*, *49*, 171–191.

Williams, M., C. M. Ryan, R. M. Rees, E. Sambane, J. Fernando, and J. Grace (2008), Carbon sequestration and biodiversity of re-growing miombo woodlands in Mozambique, *For. Ecol. Manage.*, *254*, 145–155.

Williams, R. J., G. D. Cook, A. M. Gill, and P. H. R. Moore (2009), Fire regime, fire intensity and tree survival in a tropical savanna in northern Australia, *Aust. J. Ecol.*, *24*, 50–59.

Woollen, E., C. M. Ryan, and M. Williams (2012), Carbon stocks in an African woodland landscape: Spatial distributions and scales of variation, *Ecosystems*, *15*, 804–818.

Yoda, K., T. Kira, H. Ogawa, and K. Hozumi (1963), Self-thinning in overcrowded pure stands under cultivated and natural conditions (intraspecific competition among higher plants xi), *J. Inst. Polytech.*, *14*, 107–129.